Journal of Pharmaceutical Analysis 14 (2024) 101015

Contents lists available at ScienceDirect

Journal of Pharmaceutical Analysis

journal homepage: www.elsevier.com/locate/jpa

Original article

Comparative study of trastuzumab modification analysis using mono/multi-epitope affinity technology with LC-QTOF-MS

Chengyi Zuo [a, 1], Jingwei Zhou [a, 1], Sumin Bian [b], Qing Zhang [c], Yutian Lei [d], Yuan Shen [a], Zhiwei Chen [a], Peijun Ye [a], Leying Shi [a], Mao Mu [e], Jia-Huan Qu [a, ***], Zhengjin Jiang [a, **], Qiqin Wang [a, *]

[a] Institute of Pharmaceutical Analysis, College of Pharmacy/State Key Laboratory of Bioactive Molecules and Druggability Assessment/Guangdong Province Key Laboratory of Pharmacodynamic Constituents of TCM and New Drugs Research of China, Jinan University, Guangzhou, 510632, China
[b] School of Engineering, Westlake University, Hangzhou, 310024, China
[c] The First Affiliated Hospital of Jinan University, Guangzhou, 510632, China
[d] School of Biomedical Engineering, Sun Yat-sen University, Shenzhen, Guang dong, 518107, China
[e] Guangdong Institute for Drug Control, Guangzhou, 510663, China

ARTICLE INFO

Article history:
Received 14 March 2024
Received in revised form
19 May 2024
Accepted 30 May 2024
Available online 4 June 2024

Keywords:
Monoclonal antibody
Multi-epitope affinity technology
Biotransformation analysis
LC-QTOF-MS
Breast cancer

ABSTRACT

Dynamic tracking analysis of monoclonal antibodies (mAbs) biotransformation *in vivo* is crucial, as certain modifications could inactivate the protein and reduce drug efficacy. However, a particular challenge (i.e. immune recognition deficiencies) in biotransformation studies may arise when modifications occur at the paratope recognized by the antigen. To address this limitation, a multi-epitope affinity technology utilizing the metal organic framework (MOF)@Au@peptide@aptamer composite material was proposed and developed by simultaneously immobilizing complementarity determining region (CDR) mimotope peptide (HH24) and non-CDR mimotope aptamer (CH1S-6T) onto the surface of MOF@Au nanocomposite. Comparative studies demonstrated that MOF@Au@peptide@aptamer exhibited significantly enhanced enrichment capabilities for trastuzumab variants in comparison to mono-epitope affinity technology. Moreover, the higher deamidation ratio for LC-Asn-30 and isomerization ratio for HC-Asn-55 can only be monitored by the novel bioanalytical platform based on MOF@Au@peptide@aptamer and liquid chromatography-quadrupole time of flight-mass spectrometry (LC-QTOF-MS). Therefore, multi-epitope affinity technology could effectively overcome the biases of traditional affinity materials for key sites modification analysis of mAb. Particularly, the novel bioanalytical platform can be successfully used for the tracking analysis of trastuzumab modifications in different biological fluids. Compared to the spiked phosphate buffer (PB) model, faster modification trends were monitored in the spiked serum and patients' sera due to the catalytic effect of plasma proteins and relevant proteases. Differences in peptide modification levels of trastuzumab in patients' sera were also monitored. In summary, the novel bioanalytical platform based on the multi-epitope affinity technology holds great potentials for in vivo biotransformation analysis of mAb, contributing to improved understanding and paving the way for future research and clinical applications.

1. Introduction

Therapeutic monoclonal antibodies (mAbs) have made a breakthrough in the treatment of cancer and autoimmune diseases [1–5]. However, most commercial mAbs are expressed in mammalian cell lines and undergo various enzyme-catalyzed or spontaneous modifications on the backbones or side chains, leading to post-translational modifications (PTMs) such as deamidation, isomerization, oxidation, glycosylation and glycation [6–9]. These modifications located in the paratope recognized by the antigen, such as trastuzumab LC-Asn-30 in complementarity-determining region 1 (CDR1), HC-Asn-55 in CDR2 and HC-Asp-102 in CDR3, may negatively affect binding to the target antigen, leading to the loss of drug activity, inducing undesirable changes in immunogenicity and pharmacokinetics (PK) [10–14]. In particular, major

* Corresponding author.
** Corresponding author.
*** Corresponding author.
E-mail addresses: jiahuanqu@jnu.edu.cn (J.-H. Qu), jzjjackson@hotmail.com (Z. Jiang), qiqinxtu@163.com (Q. Wang).
[1] Both authors contributed equally to this work.

https://doi.org/10.1016/j.jpha.2024.101015

modifications may accelerate after administration of mAbs to the patients. For example, HC-Asn-55 deamidation increased from 0.99% (day 0) to 2.87% (day 43), and HC-Asn-384/389 deamidation increased from 16.62% (day 0) to 38.65% (day 43) *in vivo* [15]. Therefore, understanding the modifications or biotransformation of mAbs *in vivo* is crucial for advancing drug discovery and development, which can lead to the design of more robust drug candidates with favorable *in vivo* PK properties or re-engineered to substitute labile components with more stable alternatives [16–18].

In recent years, hybrid immunoaffinity liquid chromatography-mass spectrometry (LC-MS) based on antigen functionalized materials has been developed for the analysis of mAb modifications in biological fluids [19–23]. However, *in vivo* tracking analysis of mAb modifications faces challenges due to the low mAb concentrations and complex serum matrix containing high levels of endogenous human immunoglobulin G (hIgG) [24,25]. Predictive *in vitro* models, such as phosphate buffer (PB) or serum, are attractive alternatives to *in vivo* studies, but ignore relevant proteases responsible for mAb biotransformation *in vivo* [15,26]. Therefore, some conflicting results have been reported between *in vitro* and *in vivo* models [15]. For example, Yin et al. [27] evidenced that *in vivo* mAb modifications, including C-terminal lysine removal, deamidation, pyroglutamic acid, thioether-linked heavy chain and light chain, are not fully represented by *in vitro* PB or plasma incubation. Especially, a particular challenge (i.e., immune recognition deficiencies) in biotransformation studies may arise if the paratope recognized by target antigen is modified or the modification at the CDR residues of mAb results in a loss of interaction between drug and antigen-based affinity material. To evaluate the potential bias between antigen and anti-idiotypic antibody (anti-Id) based materials for the quantitation of the related modifications, a head-to-head comparative study was performed by Zhang et al. [28] and indicated that no significantly detectable bias was found for the two capture regents. However, the authors guess that the neutralizing anti-Id and antigen may suffer the same biases (immune recognition deficiencies) because they bind to the similar regions of the antibody. Polyclonal anti-Id could significantly reduce the risk of immune recognition deficiency associated with traditional immunoaffinity materials, but inconsistency of polyclonal anti-Id lots and cross-reactivity are common problems with this class of affinity reagents. Therefore, reliable affinity technologies and bioanalytical methods are desired for precise recognition and analysis of mAb and its variants *in vivo*.

Inspired by the polyclonal anti-Id, a CDR modification-sensitive antibody (trastuzumab, first-line therapy for breast cancer) was selected as model drug in this study. Moreover, a multi-epitope affinity technology that can bind to distinct regions of trastuzumab was proposed for the precise recognition of trastuzumab and related modification variants in biological fluids. Based on the novel technology, the metal organic framework (MOF)@Au@peptide@aptamer composite material was developed by simultaneously immobilizing CDR mimotope peptide (HH24) and non-CDR mimotope aptamer (CH1S-6T) onto the surface of MOF@Au nanocomposite. Moreover, different mono-epitope recognition materials immobilized with peptide (MOF@Au@peptide) or aptamer (MOF@Au@aptamer) were successively synthesized for comparison. Comparative studies monitoring trastuzumab modifications were carried out using three types of affinity materials combined with liquid chromatography-quadrupole time of flight-mass spectrometry (LC-QTOF-MS) at the peptide mapping level. Based on the aforementioned insights, a novel bioanalytical platform based on the multi-epitope affinity technology was established, evaluated, and eventually investigated in practical applications using a series of human epidermal growth factor receptor 2 (HER2)-positive breast cancer sera.

2. Materials and methods

2.1. Materials and reagents

HHHHHHGSGSGSQLGPYELWELSH (HH24) and HHHHHHGSG SGS (HS12) peptides (98%) were synthesized by GenScript (Nanjing, China). TTTTTTGTGTCCAGGGTTCCAAGGTGCTTCGTGGACAC (CH1S-6T) and polyA-30 aptamers were synthesized by Sangon Biotech (Shanghai, China). Trastuzumab was purchased from Roche Pharmaceutical Co., Ltd. (Shanghai, China). Sequencing grade modified trypsin was from Promega (Mannheim, Germany). Tris(hydroxymethyl)aminomethane (Tris, 99.8%), urea (99%), DL-Dithiothreitol (DTT, 99%), sodium azide (NaN_3, 98%), monosodium phosphate (NaH_2PO_4, 99%), disodium hydrogen phosphate (Na_2HPO_4, 99%), ε-aminocaproic acid (EACA), triethylene tetramine (TETA), and hydroxypropyl methyl cellulose (HPMC) were purchased from Aladdin Chemicals (Shanghai, China). 2-Iodoacetamide (IAM, 97%) was from Energy Chemical (Shanghai, China). Hydrochloric acid (HCl, 36%) was obtained from Guangzhou Chemical Reagent Factory (Guangzhou, China). Formic acid (FA, MS grade) was bought from Macklin (Shanghai, China). Acetonitrile (ACN, MS grade) was from Merck (Darmstadt, Germany). Distilled water used in the mobile phase was purchased from Watson's Food and Beverage Co., Ltd (Guangzhou, China). Ultrapure water utilized for all the solution preparations was obtained from an ultrapure water polishing system (Omni-A, Xiamen, China). Serum of healthy individuals was provided by the First Affiliated Hospital of Jinan University (Guangzhou, China). Breast cancer patients' sera were provided by the Dongguan People's Hospital (Dongguan, Guangdong, China). All of the clinical samples have got the ethics approval (Approval number: JNUKY-2023-0080).

2.2. Development of mono/multi-epitope affinity materials

The MOF@Au@peptide@aptamer composite material was developed by simultaneously immobilizing CDR mimotope peptide (HH24) and non-CDR mimotope aptamer (CH1S-6T) onto the surface of MOF@Au nanocomposite (Fig. S1). Additionally, MOF@Au@peptide was synthesized by immobilizing HH24 onto the surface of MOF@Au nanocomposite and blocking with polyA-30, while MOF@Au@aptamer was synthesized by immobilizing CH1S-6T onto the surface of MOF@Au nanocomposite and blocking with HS12. A more detailed preparation process can be found in the Supplementary data [29,30].

2.3. In vitro incubation of trastuzumab in PB and human serum

Trastuzumab was spiked into 20 mM PB (pH 7.4) or human serum to achieve a final concentration of 1 mg/mL. The samples were incubated at 37 °C in the presence of 0.2% sodium azide, with 1 mL of each sample being collected at the interval of 0, 4, 7, 14 and 21 days. Subsequently, all the collected samples were stored at −80 °C until pretreatment for analysis.

2.4. Capillary zone electrophoresis (CZE) analysis of the incubated trastuzumab in PB

CZE analysis was performed on a PA 800 Plus CE system using the 32 Karat™ 8.0 Software from AB SCIEX (Foster City, CA, USA). The temperature of the autosampler and capillary cartridge were set at 10 °C and 20 °C, respectively. The running buffer was made up of 4.275 mL buffer A (400 mM EACA, 2 mM TETA, pH 5.7) and 450 μL buffer B (1% HPMC). Polymicro bare fused silica capillaries (50 cm total length, 40 cm effective length, 50 μm ID) were obtained from Photonlines (Saint-Germain-en-Laye, France). The

capillary was flushed with 0.1 M NaOH, 0.1 M HCl and water for 5 min at 20 psi prior to the first use, and then equilibrated with the running buffer for 20 min between runs. Incubated trastuzumab samples were injected for 30 s at 2 psi. The separation time and voltage were 32 min and 28 kV. The monitoring wavelength of the photodiode array detector was set at 280 nm with a data sampling rate of 4 Hz.

2.5. Secondary structure analysis of the incubated trastuzumab in PB

A Chirascan circular dichroism (CD) spectrometer (Applied Photophysics Ltd., Leatherhead, UK) was applied to analyze the secondary structure of trastuzumab during the incubation period in PB. To mitigate interference, phosphate and sodium azide in PB samples were removed using a 10 kDa MWCO filter (Amicon Millipore Corporation, Bedford, MA, USA). Subsequently, the samples were diluted with purified water to a 3 μM solution. Measurements of the buffer and trastuzumab samples were performed using an ultraviolet spectrophotometer at 25 °C, scanning from 195 to 260 nm with a bandwidth of 1 nm. The buffer spectrum was subtracted from the sample spectra and converted to molar ellipticity. Deconvolution was performed to estimate the secondary structure of trastuzumab spectra. The secondary structure was calculated considering the molecular weight of 148 kDa for trastuzumab and a total number of 1,328 amino acids.

2.6. Purification of trastuzumab from breast cancer patients' sera

The serum samples were collected from five trastuzumab-treated patients with HER2-positive breast cancer, and stored at −80 °C before analysis. The samples were thawed at 4 °C for 1 h, and then centrifuged at 3,000 rpm for 20 min. 200 μL supernatant solution diluted threefold was mixed and incubated with 50 μL MOF@Au@peptide@aptamer for 1 h, followed by centrifugation at 10,000 rpm for 5 min to collect the precipitation. Washing buffer (10 mM Tris-HCl, pH 7.0) was applied to remove the impurities for 3 times, with each time using 200 μL. Finally, 200 μL elution buffer (0.1% FA, 25% ACN) was added and shaken for 2 h to obtain the target trastuzumab.

2.7. Sample preparation for peptide mapping analysis

Firstly, the elution buffer of the samples was exchanged to digestion buffer (10 M urea in 100 mM Tris-HCl, pH 8.0) using a 10 kDa MWCO filter according to the manufacturer's instructions. Reduction was achieved by the addition of 0.5 M DTT to a final concentration of 10 mM, followed by incubation at 50 °C for 30 min. Alkylation was performed by adding 1 M IAM to a final concentration of 20 mM and kept from light for 30 min at room temperature. Then the buffer was diluted with 100 mM Tris-HCl (pH 8.0) to a concentration of urea less than 1 M. Sequencing grade modified trypsin was added at a 1:25 (enzyme:trastuzumab) mass ratio, and digestion was allowed to proceed for a 3 h water bath at 37 °C. Finally, 5% FA was added to a final concentration of 0.5% to terminate the digestion.

2.8. LC-QTOF-MS analysis

The analyses were performed on an ExionLC™ AD system coupled to a quadrupole time-of-flight mass spectrometer (X500R Q-TOF, AB SCIEX). 20 μL of each sample was injected into the system and separated with an ACQUITY UPLC® BEH C18 column (2.1 mm × 150 mm, 1.7 μm; Waters Corporation, Milford, MA, USA) at 60 °C. The separations were carried out using 0.1% FA in water as mobile phase A and 0.1% FA in ACN as mobile phase B at a flow rate of 0.2 mL/min. The gradient started at 2% B for 2 min, then gradually increased to 40% B at 100 min, followed by a quick decrease to 90% B at 103 min, where it remained constant for 7 min. Subsequently, it was reverted to 2% B at 111 min and kept for 9 min to allow for equilibration.

The mass spectrometer was equipped with a TurboIonSpray (AB SCIEX, Foster City, CA, USA) ion source and operated employing electrospray ionization (ESI) source in positive mode. The ionization settings were as follows: curtain gas, ion source gas 1 (nebulizing gas) and ion source gas 2 (heater gas) pressures were set at 40, 50 and 50 psi, respectively; source temperature was set at 500 °C; ion spray voltage was set at 5,500 V.

Mass acquisition was performed using TOF-MS and TOF-MS/MS scan with information-dependent acquisition (IDA) experiment. The parameters used in TOF-MS scan were as follows: TOF mass range, 100–2,000 Da; accumulation time, 0.15 s; declustering potential (DP), 80 V; collision energy (CE), 10 V. TOF-MS/MS scan was performed under the following conditions: maximum candidate ions, 15; intensity threshold, 100 cps; TOF mass range, 50–2,000 Da; accumulation time, 0.06 s; charge state, 1 to 7; with dynamic background subtraction and dynamic CE for MS/MS.

Data acquisition and analysis were controlled by SCIEX OS software (version 2.1, AB SCIEX). The modified and unmodified peptides with the highest charge response in the extracted ion chromatograms (XICs) were selected for relative quantification.

3. Results and discussion

3.1. Peptide mapping analysis

For the modification or biotransformation analysis of mAb in complex biological samples, a reliable analytical workflow was firstly developed and evaluated by LC-QTOF-MS combined with trypsin digestion. Fig. 1A showed the total ion chromatogram (TIC) for the TOF-MS and TOF-MS/MS of the tryptic peptides of trastuzumab. Figs. 1B–F exhibited the XICs of peptides and the corresponding modified peptides in the variable region of trastuzumab. All the chromatographic peaks achieved baseline separation with a long-time gradient elution, which was sufficient for relative quantification.

Among these, asparagine (Asn) deamidation and isomerization have been widely studied as critical quality attributes, as they could affect the binding affinity of antibody to antigen if located in CDR [31,32]. As can be seen in Figs. 2A and B, the deamidation of Asn in some key sites (such as LC-Asn-30, HC-Asn-55 and HC-Asn-84) produced a mass increase of approximately 0.98 Da for the modified peptides. Methionine (Met) or tryptophan oxidation could result in conformational changes of mAb, which affect antibody binding to fragment crystallizable (Fc) receptors and antigens, or alter mAb stability and half-life [33]. Figs. 2C and D illustrate the molecular mass of the oxidation products increased by about 15.99 Da due to the addition of one oxygen atom, such as LC-Met-4, HC-Met-83 and HC-Met-107. In addition, N-terminal glutamate (Glu) cyclization to form pyroglutamate (pGlu) generates charge heterogeneity for mAb [34,35]. If the N-terminal residues are located in the variable region or near the CDR, the pGlu formation may affect target binding [36]. As shown in Figs. 2E and F, the mass reduction of 18.01 Da implied the loss of one H_2O molecule in the process of cyclization. Collectively, the analytical workflow exhibited good separation selectivity and MS intensity for the identification and analysis of modified peptides in the target mAb.

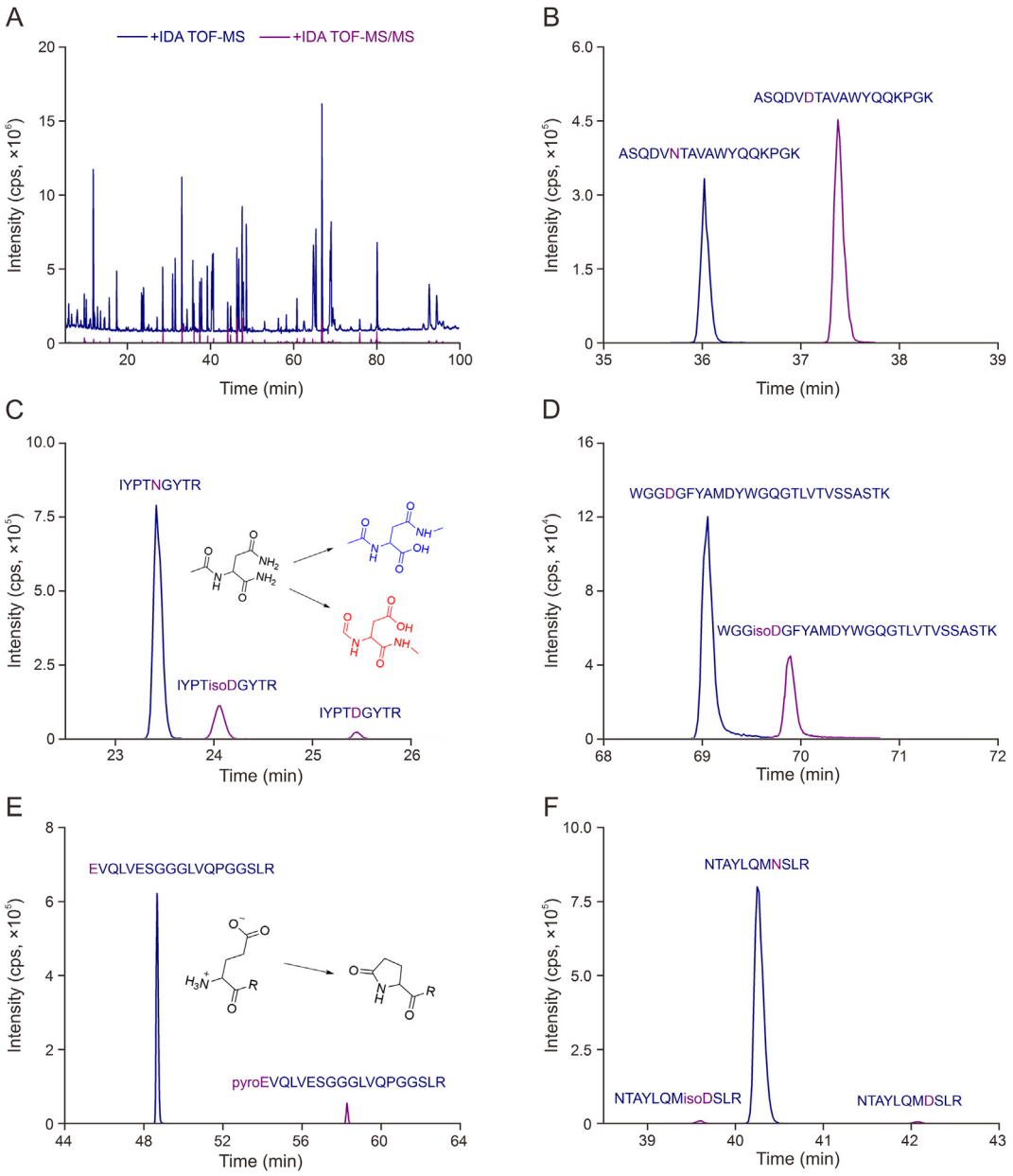

Fig. 1. Peptide mapping analysis of trastuzumab incubated in phosphate buffer for 21 days. (A) Total ion chromatogram for the mass spectrometry (MS) and tandem mass spectrometry (MS/MS). (B) Extracted ion chromatogram (XIC) of ASQDVNTAVAWYQQKPGK+3 and the corresponding light chain (LC) N30 deamidation peptide in complementarity-determining region (CDR) of the variable region. (C) XIC of IYPTNGYTR+2 and the corresponding heavy chain (HC) N55 isomerization and deamidation peptides in CDR of the variable region. (D) XIC of WGGDGFYAMDYWGQGTLVTVSSASTK+3 and the corresponding HC D102 isomerization peptide in CDR of the variable region. (E) XIC of EVQLVESGGGLVQPGGSLR+3 and the corresponding HC E1 cyclization peptide in non-CDR of the variable region. (F) XIC of NTAYLQMNSLR+2 and the corresponding HC N84 isomerization and deamidation peptides in non-CDR of the variable region.

3.2. Comparative study of multi-epitope affinity technology versus mono-epitope affinity technologies

To select the most suitable affinity technology for precise enrichment of trastuzumab and its variants, the MOF@Au@peptide, MOF@Au@aptamer and MOF@Au@peptide@aptamer were synthesized and compared (Fig. 3). The modification sites and ratios in CDR of the incubated trastuzumab were identified and compared by three different analytical methods, and the key modification sites of trastuzumab selected for analysis were shown in Fig. 4A. Firstly, the highest enrichment recovery (93%) for trastuzumab was achieved of MOF@Au@peptide@aptamer in comparison to that of MOF@Au@peptide (70%), and MOF@Au@aptamer (90%), as depicted in Fig. 4B. Besides, over 98% sequence coverage was obtained for all the enriched trastuzumab by three affinity technologies (Fig. 4C). These peptide sequences and positions of trastuzumab are listed in Tables S1 and S2 and the sequence coverage information of trastuzumab enriched by these three affinity materials is summarized in Fig. S2.

Secondly, a pioneering bioanalytical platform was established by combining various affinity technologies, trypsin digestion and LC-QTOF-MS. The direct analysis results of the incubated trastuzumab were used as the control group. As depicted in Fig. S3, no significant difference was observed for HC-N55-Dea, HC-N84-Dea, HC-N84-Iso, HC-D102-Iso, HC-N318-Dea and HC-N384/392/393-Dea from all the analytical results. However, as shown in Figs.

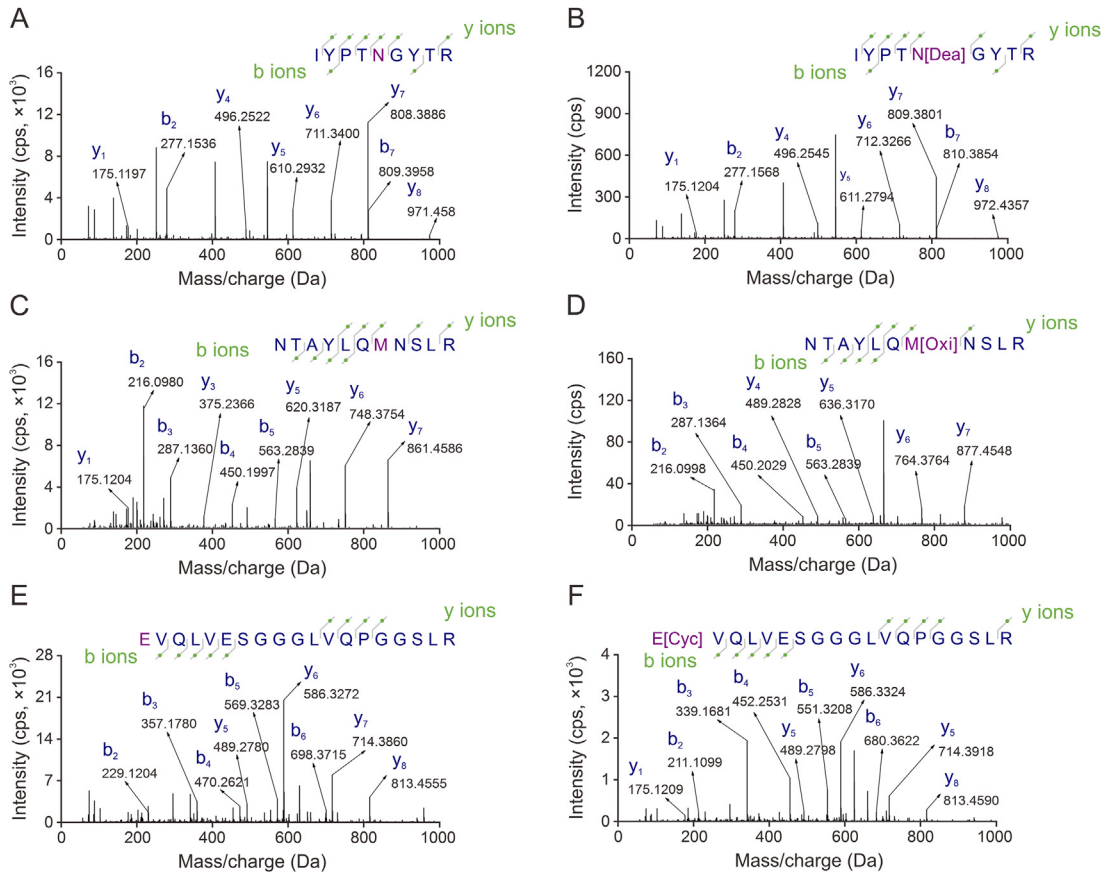

Fig. 2. Tandem mass spectrometry (MS/MS) spectra of the analyzed peptides. (A, B) MS/MS spectra of IYPTNGYTR+2 and the corresponding heavy chain (HC) N55 deamidation (Dea) peptide. (C, D) MS/MS spectra of NTAYLQMNSLR+2 and the corresponding HC M83 oxidation (Oxi) peptide. (E, F) MS/MS spectra of EVQLVESGGGLVQPGGSLR+3 and the corresponding HC E1 cyclization (Cyc) peptide.

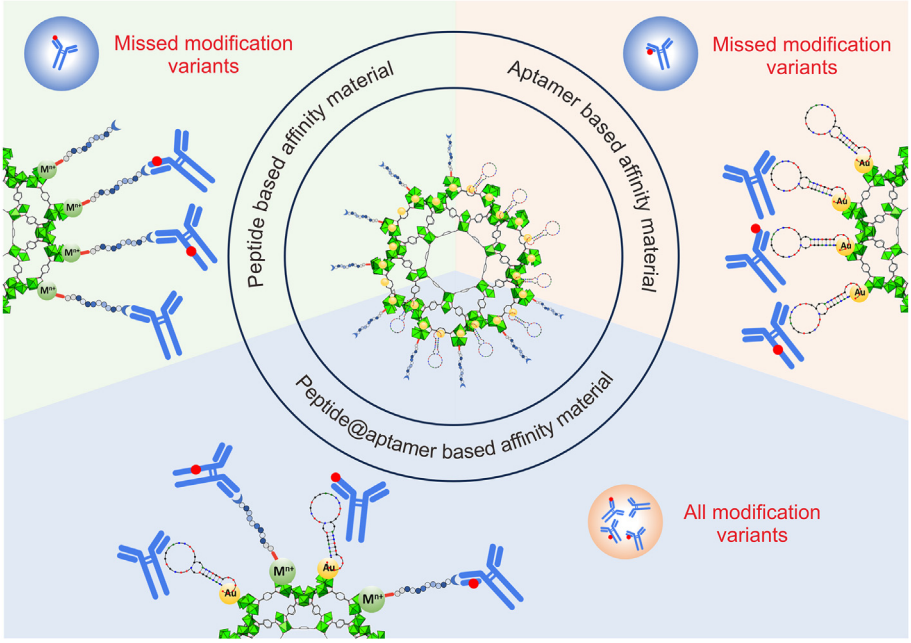

Fig. 3. Schematic illustration of comparative study of multi-epitope versus mono-epitope affinity technologies.

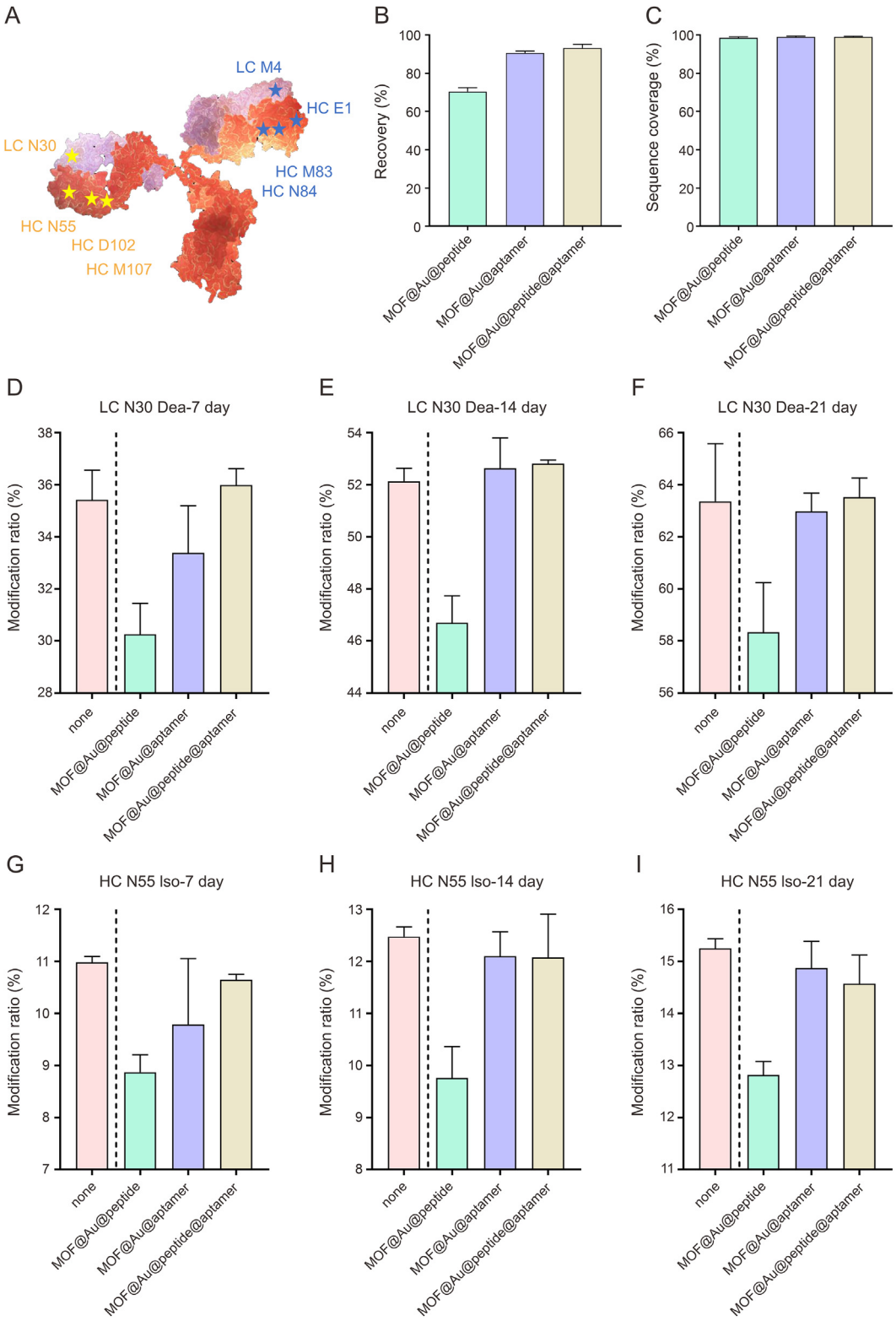

Fig. 4. Comparative study of multi-epitope affinity technology versus mono-epitope affinity technologies. (A) The key modification sites of trastuzumab selected for analysis. (B, C) Comparisons of recovery (B) and sequence coverage (C) of trastuzumab captured by metal organic framework (MOF)@Au@peptide, MOF@Au@aptamer and MOF@Au@peptide@aptamer. (D–I) Comparative results of light chain (LC) N30 deamidation (Dea) (D–F) and heavy chain (HC) N55 isomerization (Iso) (G–I) ratios of trastuzumab incubated for 7, 14 and 21 days after pretreatment with MOF@Au@peptide, MOF@Au@aptamer, MOF@Au@peptide@aptamer, with none as the control.

4D–F, compared to analytical methods based on the mono-epitope affinity technologies, the multi-epitope affinity technology revealed a higher deamidation ratio (35.99%) for Asn30 (located in the CDR1 of light chain), which closely resembled the direct analysis results obtained from trastuzumab incubated for 7 days. Similar phenomenon was also observed for the isomerization analysis of Asn55 at the CDR2 of heavy chain (Figs. 4G–I). These results highlight the superior performances of multi-epitope affinity technology in overcoming the immune recognition deficiencies of traditional affinity technology, with enhanced enrichment recovery and accurate modification monitoring.

Thirdly, a series of trastuzumab spiked in PB over an extended period of time (0, 4, 7, 14 and 21 days) were analyzed from the intact protein level. As shown in Fig. 5A, after incubation in PB for 21 days, the acidic charge variants were rapidly increased with a corresponding decrease in the main peak of trastuzumab. The increase of acid charge variants could be derived from the formation of Asn deamidation, aspartic acid isomerization, Met oxidation and N-terminal glutamic acid cyclization [37]. However, the secondary structure of the incubated trastuzumab remained largely intact over the course of 21 days (Fig. 5B), indicating that these variants have a limited impact on the secondary structure of target mAb.

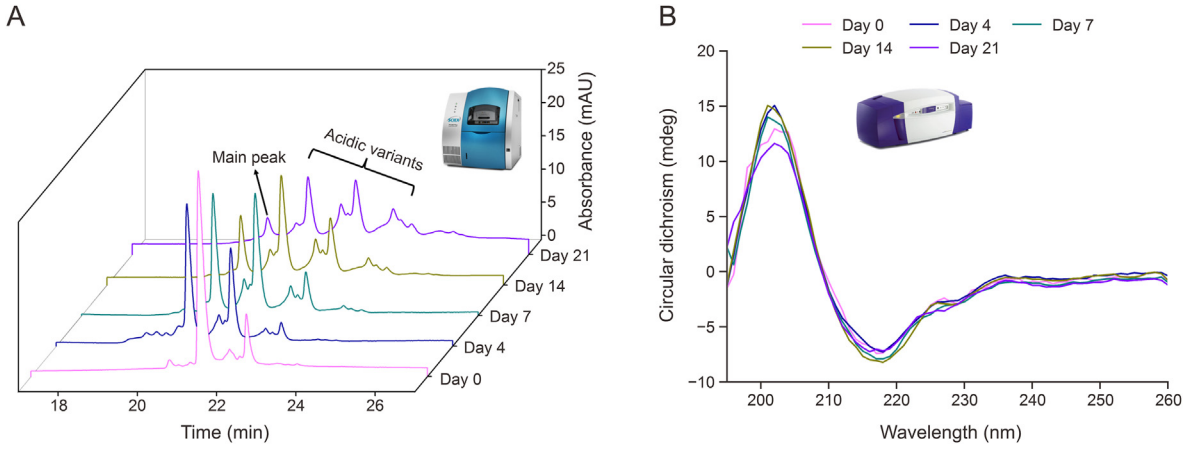

Fig. 5. Variants analyses of the incubated trastuzumab from the intact protein level. (A) Capillary zone electrophoresis analysis and (B) circular dichroism spectra of trastuzumab incubated in phosphate buffer for 0, 4, 7, 14 and 21 days.

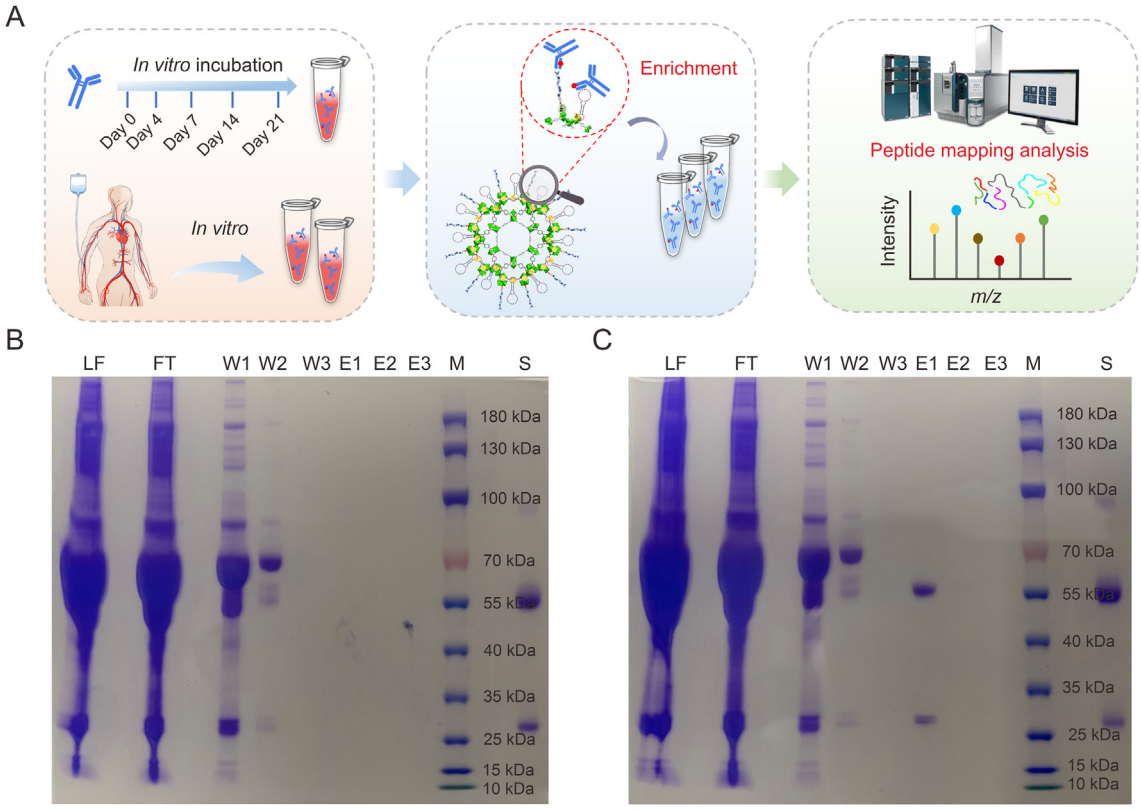

Fig. 6. Specificity of the multi-epitope affinity technology. (A) Workflow of the analysis in complex biological fluids. (B, C) Enrichment of trastuzumab in blank (B) and spiked sera (C) using metal organic framework (MOF)@Au@peptide@aptamer. Sodium dodecyl sulfate polyacrylamide gel electrophoresis analysis (reducing condition) with different lanes as follows: LF: loading fraction; FT: flow through; W: washing fractions; E: elution fractions; M: protein marker; S: standard trastuzumab.

3.3. Evaluation and application of the bioanalytical platform based on the multi-epitope affinity technology

Leveraging the above superior performances, the novel bioanalytical platform based on the multi-epitope affinity technology was further employed for the tracking analysis of trastuzumab modifications in an *in vitro* spiked serum model. Compared to the PB model, there are high levels of endogenous IgGs at the concentration of 7–18 mg/mL in serum, which is 100–1,000 times the concentration of circulating mAb in a typical pharmacokinetic study [38–41]. Therefore, affinity technology with high specificity and anti-fouling ability was urgently desired. Fig. 6A illustrates the analytical workflow based on the novel platform in complex biological fluids, such as spiked serum and patients' sera. As depicted in Fig. 6B, the sodium dodecyl sulfate polyacrylamide gel electrophoresis (SDS-PAGE) analysis revealed the absence of interference proteins in the elution fractions of blank serum. In contrast, the elution fraction of the spiked serum exhibited two characteristic peaks (Fig. 6C), corresponding to the heavy and light chains of trastuzumab, respectively.

Moreover, for the detection of characteristic peptide segments, the interference from blank serum became negligible following

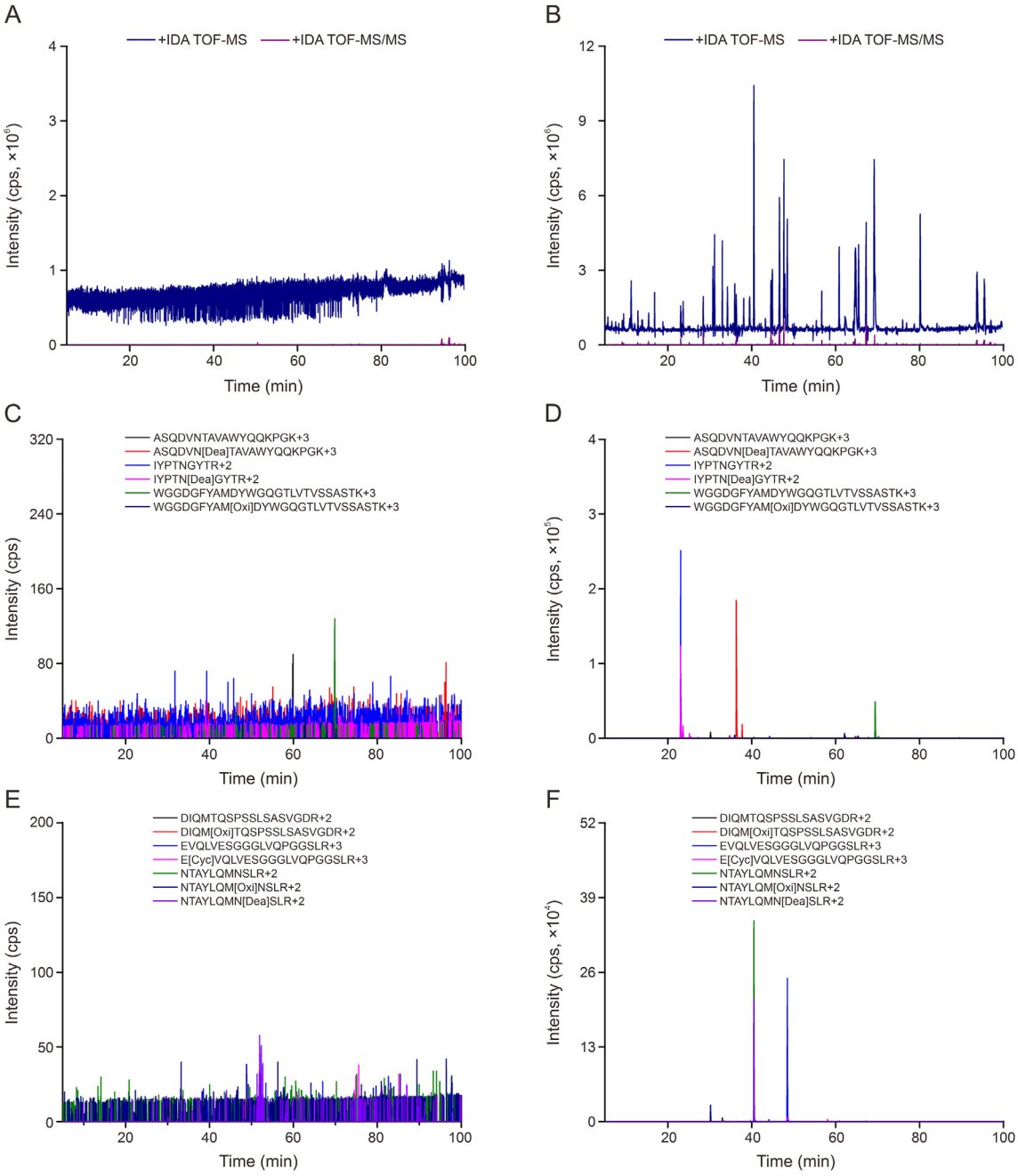

Fig. 7. Evaluation of the bioanalytical platform based on the multi-epitope affinity technology. Total ion chromatograms for the mass spectrometry (MS) and tandem mass spectrometry (MS/MS) of (A) blank and (B) spiked sera. Extracted ion chromatograms for the complementarity-determining region (CDR) peptides of (C) blank and (D) spiked sera. Extracted ion chromatograms for the non-CDR peptides of (E) blank and (F) spiked sera. All the blank and spiked sera were pretreated with metal organic framework (MOF) @Au@peptide@aptamer.

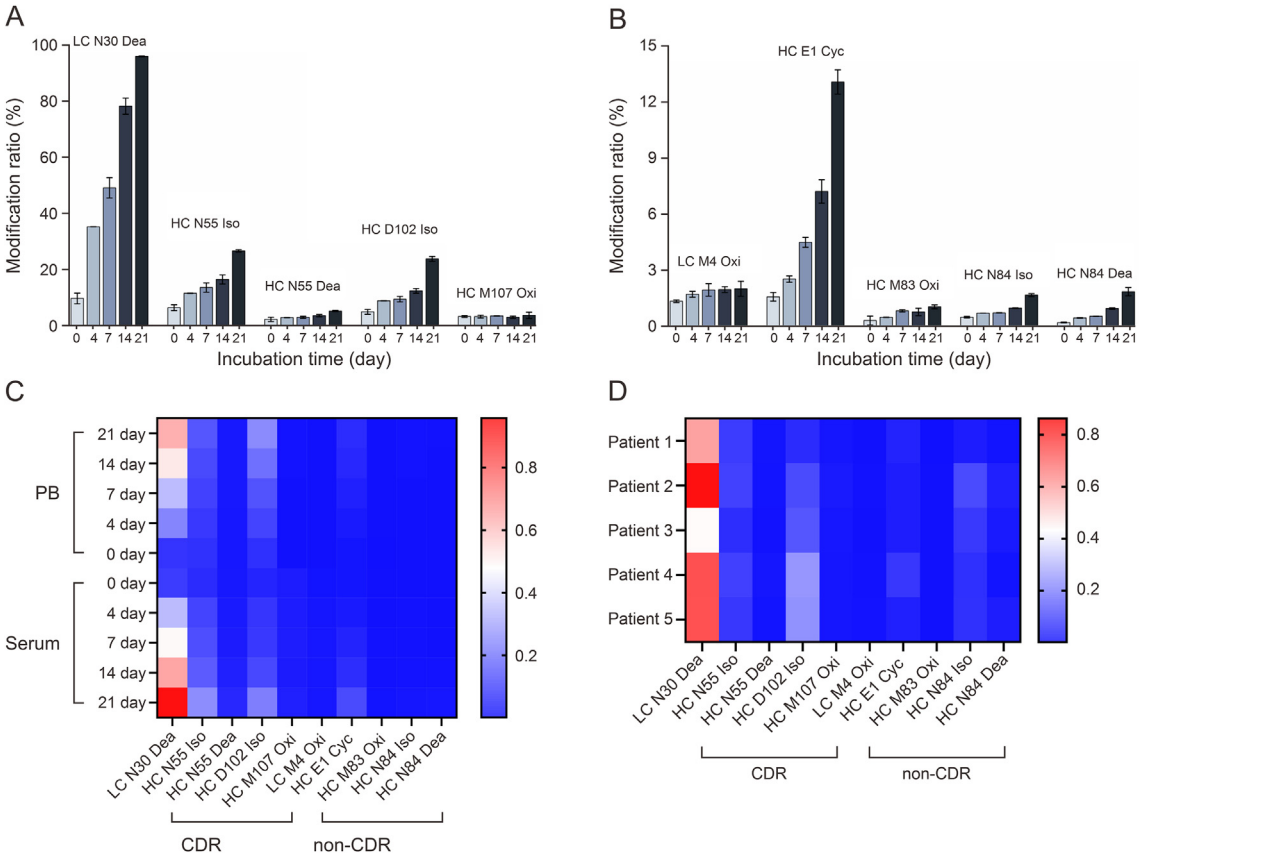

Fig. 8. Application of the bioanalytical platform based on the multi-epitope affinity technology. (A, B) Biotransformation analysis for complementarity-determining region (CDR) (A) and non-CDR (B) amino acid sites of trastuzumab incubated in serum over 21 days. (C) Comparative results for the modification trends of trastuzumab incubated in phosphate buffer (PB) and serum over 21 days. (D) Biotransformation analysis of trastuzumab in breast cancer patients' sera. LC: light chain; HC: heavy chain; Dea: deamidation; Iso: isomerization; Oxi: oxidation; Cyc: cyclization.

affinity pretreatment (Figs. 7A, C and E). In contrast, spiked serum exhibited a significant mass response intensity for the target peptides following affinity pretreatment (Figs. 7B, D and F). These results demonstrated the excellent specificity of the multi-epitope affinity technology for trastuzumab and its excellent antifouling ability towards interfering proteins in serum, thus overcoming the limitations associated with nonspecific adsorption observed with protein A/G/L [42] and KH19 based affinity materials [43].

To further investigate the application potential of the bioanalytical platform, dynamic tracking analysis of trastuzumab modifications in spiked serum was performed. As described in Figs. 8A and B, incubation in serum for 21 days led to a rapid increase in the deamidation level of LC-Asn-30 to aspartic acid, from 9.64% (day 0) to 95.72% (day 21), while the deamidation ratio of HC-Asn-55 to aspartic acid and isomerization to isoaspartic acid showed moderate changes, such as from 2.20% (day 0) to 5.17% (day 21) for deamidation and from 6.36% (day 0) to 26.55% (day 21) for isomerization. Similarly, slow changing trends were observed for the isomerization of HC-Asp-102 and HC-Asn-84, the deamidation of HC-Asn-84, and the oxidation of HC-Met-83, LC-Met-4, and HC-Met-107. However, the conversion of Asn55 to aspartic acid (Asp55) and the concomitant isomerization to isoaspartic acid (isoAsp55) resulted in a significant decrease of bioactivity (>70%) due to a reduction in antigen binding affinity [44]. In addition, compared to the analytical results of the spiked PB model (Fig. S4), more profound modification trends in deamidation, isomerization and pyroglutamic acid cyclization of key amino acid sites were observed in the spiked serum model (Fig. 8C), which may be attributed to the catalytic effect of plasma proteins and relevant proteases [45]. In summary, the bioanalytical platform demonstrated great potential for exploring modification sites and trends of the target mAb in complex biological fluids.

Finally, this bioanalytical platform was applied for *in vivo* analysis of trastuzumab biotransformation in HER2 positive patients' sera. Blood samples were collected from five breast cancer patients after trastuzumab administration. As summarized in Fig. 8D, all the key modification sites of trastuzumab could be identified using this platform in patients' sera. Moreover, similar modification trends were observed between spiked serum and patients' sera. However, diverse modification ratios across amino acid sites were observed among different patients. This may be attributed to the factors like patients' age, physical function, dietary habits and combination medication. These findings may reveal the metabolic process of trastuzumab after administration in actual patients, which is meaningful for the early development and biotransformation research of therapeutic mAbs and related products. Therefore, this novel analytical platform holds great potential for studying the biotransformation of therapeutic mAbs in clinical settings.

4. Conclusions

In this study, to overcome the immune recognition deficiencies associated with traditional affinity methods, a multi-epitope affinity technology (MOF@Au@peptide@aptamer composite material) was proposed and developed. Comparative studies revealed a significantly improved enrichment capability for trastuzumab

when utilizing this composite material, surpassing that of mono-epitope affinity technology (MOF@Au@peptide or MOF@Au@aptamer). Notably, the novel bioanalytical platform based on MOF@Au@peptide@aptamer enabled the monitoring of higher deamidation ratio for LC-Asn-30 and isomerization ratio for HC-Asn-55. Leveraging these superior attributes, the novel bioanalytical platform was successfully employed for the tracking analysis of trastuzumab modifications across diverse biological systems. Compared to the spiked PB model, faster modification trends were observed in the spiked serum and patients' sera due to the catalytic effect of plasma proteins and relevant proteases. In conclusion, these findings not only provide an innovative bioanalytical platform for dynamic *in vivo* biotransformation analysis of target mAb, but also have the potential to extend the scope of this field beyond its current academic boundaries.

CRediT authorship contribution statement

Chengyi Zuo: Data curation, Formal analysis, Investigation, Methodology, Validation, Writing – original draft. **Jingwei Zhou:** Conceptualization, Data curation, Formal analysis, Methodology, Validation. **Sumin Bian:** Formal analysis, Validation, Writing – review & editing. **Qing Zhang:** Validation, Writing – review & editing. **Yutian Lei:** Investigation, Methodology. **Yuan Shen:** Data curation, Methodology. **Zhiwei Chen:** Validation, Visualization. **Peijun Ye:** Formal analysis, Validation. **Leying Shi:** Data curation, Validation. **Mao Mu:** Data curation, Validation. **Jia-Huan Qu:** Visualization, Writing – review & editing. **Zhengjin Jiang:** Funding acquisition, Resources, Supervision. **Qiqin Wang:** Funding acquisition, Supervision, Writing – review & editing.

Declaration of competing interest

As an editorial board member, Zhengjin Jiang recused himself from all review processes related to this article to ensure the fairness and objectivity of the review. Other authors declare that there are no conflicts of interest.

Acknowledgments

This work was supported by the National Natural Science Foundation of China (Grant Nos.: 82373829, 82273893, and 82173773), the Natural Science Foundation of Guangdong Province, China (Grant Nos.: 2021A1515220099, and 2022A1515011576), the High-End Foreign Experts Project, China (Grant No.: G2021199005L), and the Science and Technology Program of Guangdong Provincial Medical Products Administration, China (Grant Nos.: 2023TDZ11, and 2022ZDB04).

Appendix A. Supplementary data

Supplementary data to this article can be found online at https://doi.org/10.1016/j.jpha.2024.101015.

References

[1] G. Pantaleo, B. Correia, C. Fenwick, et al., Antibodies to combat viral infections: Development strategies and progress, Nat. Rev. Drug Discov. 21 (2022) 676–696.
[2] H. Kaplon, S. Crescioli, A. Chenoweth, et al., Antibodies to watch in 2023, mAbs 15 (2023), 2153410.
[3] D. Corti, L.A. Purcell, G. Snell, et al., Tackling COVID-19 with neutralizing monoclonal antibodies, Cell 184 (2021) 4593–4595.
[4] P. Zhu, S.-Y. Li, J. Ding, et al., Combination immunotherapy of glioblastoma with dendritic cell cancer vaccines, anti-PD-1 and poly I:C, J. Pharm. Anal. 13 (2023) 616–624.
[5] J.-J. Zhang, C.-G. Song, M. Wang, et al., Monoclonal antibody targeting mu-opioid receptor attenuates morphine tolerance via enhancing morphine-induced receptor endocytosis, J. Pharm. Anal. 13 (2023) 1135–1152.
[6] C.T. Walsh, S. Garneau-Tsodikova, G.J. Gatto, Protein posttranslational modifications: The chemistry of proteome diversifications, Angew. Chem. Int. Ed. 44 (2005) 7342–7372.
[7] J.C. Tran, D. Tran, A. Hilderbrand, et al., Automated affinity capture and on-tip digestion to accurately quantitate *in vivo* deamidation of therapeutic antibodies, Anal. Chem. 88 (2016) 11521–11526.
[8] F. Cymer, H. Beck, A. Rohde, et al., Therapeutic monoclonal antibody N-glycosylation-structure, function and therapeutic potential, Biologicals 52 (2018) 1–11.
[9] Y. Mimura, R. Saldova, Y. Mimura-Kimura, et al., Micro-heterogeneity of antibody molecules, Exp. Suppl. 112 (2021) 1–26.
[10] C. Nowak, A. Tiwari, H. Liu, Asparagine deamidation in a complementarity determining region of a recombinant monoclonal antibody in complex with antigen, Anal. Chem. 90 (2018) 6998–7003.
[11] Y. Yan, H. Wei, Y. Fu, et al., Isomerization and oxidation in the complementarity-determining regions of a monoclonal antibody: A study of the modification-structure-function correlations by hydrogen-deuterium exchange mass spectrometry, Anal. Chem. 88 (2016) 2041–2050.
[12] B. Beyer, M. Schuster, A. Jungbauer, et al., Microheterogeneity of recombinant antibodies: Analytics and functional impact, Biotechnol. J. 13 (2018), 1700476.
[13] J.A. Pavon, L. Xiao, X. Li, et al., Selective tryptophan oxidation of monoclonal antibodies: Oxidative stress and modeling prediction, Anal. Chem. 91 (2019) 2192–2200.
[14] A. Beck, E. Wagner-Rousset, D. Ayoub, et al., Characterization of therapeutic antibodies and related products, Anal. Chem. 85 (2013) 715–736.
[15] N. Yang, Q. Tang, P. Hu, et al., Use of *in vitro* systems to model *in vivo* degradation of therapeutic monoclonal antibodies, Anal. Chem. 90 (2018) 7896–7902.
[16] S. Schadt, S. Hauri, F. Lopes, et al., Are biotransformation studies of therapeutic proteins needed? Scientific considerations and technical challenges, Drug Metab. Dispos. 47 (2019) 1443–1456.
[17] P. Bults, R. Bischoff, H. Bakker, et al., LC-MS/MS-based monitoring of *in vivo* protein biotransformation: Quantitative determination of trastuzumab and its deamidation products in human plasma, Anal. Chem. 88 (2016) 1871–1877.
[18] Y. Li, M. Monine, Y. Huang, et al., Quantitation and pharmacokinetic modeling of therapeutic antibody quality attributes in human studies, mAbs 8 (2016) 1079–1087.
[19] Y. Lei, Y. Shen, C. Zuo, et al., Emerging affinity ligands and support materials for the enrichment of monoclonal antibodies, Trends Anal. Chem. 157 (2022), 116744.
[20] M.J. Suh, J.B. Powers, C.M. Daniels, et al., Enhanced pharmacokinetic bioanalysis of antibody-drug conjugates using hybrid immunoaffinity capture and microflow LC-MS/MS, AAPS J 25 (2023), 68.
[21] L. Dong, N. Bebrin, K. Piatkov, et al., An automated multicycle immunoaffinity enrichment approach developed for sensitive mouse IgG1 antibody drug analysis in mouse plasma using LC/MS/MS, Anal. Chem. 93 (2021) 6348–6354.
[22] F. Yin, D. Adhikari, M. Sun, et al., Bioanalysis of an antibody drug conjugate (ADC) PYX-201 in human plasma using a hybrid immunoaffinity LC-MS/MS approach, J. Chromatogr. B. 1223 (2023), 123715.
[23] C. Zhu, H. Han, Z. Chen, et al., Tetrapeptide-based mimotope affinity monolith for the enrichment and analysis of anti-HER2 antibody and antibody-drug conjugate, Anal. Chim. Acta 1246 (2023), 340892.
[24] A. Gonzalez-Quintela, R. Alende, F. Gude, et al., Serum levels of immunoglobulins (IgG, IgA, IgM) in a general adult population and their relationship with alcohol consumption, smoking and common metabolic abnormalities, Clin. Exp. Immunol. 151 (2007) 42–50.
[25] M.A. French, G. Harrison, Serum IgG subclass concentrations in healthy adults: A study using monoclonal antisera, Clin. Exp. Immunol. 56 (1984) 473–475.
[26] L. Lu, X. Liu, C. Zuo, et al., *In vitro/in vivo* degradation analysis of trastuzumab by combining specific capture on HER2 mimotope peptide modified material and LC-QTOF-MS, Anal. Chim. Acta 1225 (2022), 340199.
[27] S. Yin, C.V. Pastuskovas, L.A. Khawli, et al., Characterization of therapeutic monoclonal antibodies reveals differences between *in vitro* and *in vivo* time-course studies, Pharm. Res. 30 (2013) 167–178.
[28] Y. Zhang, S.-L. Wu, Y. Li, Comparative study of profiling post-translational modifications of a circulating antibody drug in human with different capture reagents, Biologicals 45 (2017) 93–95.
[29] S. Bauer, C. Serre, T. Devic, et al., High-throughput assisted rationalization of the formation of metal organic frameworks in the Iron(III) amino-terephthalate solvothermal system, Inorg. Chem. 47 (2008) 7568–7576.
[30] Y. Hu, H. Cheng, X. Zhao, et al., Surface-enhanced Raman scattering active gold nanoparticles with enzyme-mimicking activities for measuring glucose and lactate in living tissues, ACS Nano 11 (2017) 5558–5566.
[31] C. Nowak, A. Tiwari, H. Liu, Asparagine deamidation in a complementarity determining region of a recombinant monoclonal antibody in complex with antigen, Anal. Chem. 90 (2018) 6998–7003.
[32] R. Zeunik, A.F. Ryuzoji, A. Peariso, et al., Investigation of immune responses to oxidation, deamidation, and isomerization in therapeutic antibodies using preclinical immunogenicity risk assessment assays, J. Pharm. Sci. 111 (2022) 2217–2229.

[33] Y. Wang, X. Li, Y.-H. Liu, et al., Simultaneous monitoring of oxidation, deamidation, isomerization, and glycosylation of monoclonal antibodies by liquid chromatography-mass spectrometry method with ultrafast tryptic digestion, mAbs 8 (2016) 1477–1486.
[34] M. Cao, N.D. Mel, J. Wang, et al., Characterization of N-terminal glutamate cyclization in monoclonal antibody and bispecific antibody using charge heterogeneity assays and hydrophobic interaction chromatography, J. Pharm. Sci. 111 (2022) 335–344.
[35] Z. Liu, Y. Cao, L. Zhang, et al., In-depth characterization of mAb charge variants by on-line multidimensional liquid chromatography-mass spectrometry, Anal. Chem. 95 (2023) 7977–7984.
[36] Y.D. Liu, A.M. Goetze, R.B. Bass, et al., N-terminal glutamate to pyroglutamate conversion *in vivo* for human IgG2 antibodies, J. Biol. Chem. 286 (2011) 11211–11217.
[37] A.B. Joshi, M. Sawai, W.R. Kearney, et al., Studies on the mechanism of aspartic acid cleavage and glutamine deamidation in the acidic degradation of glucagon, J. Pharm. Sci. 94 (2005) 1912–1927.
[38] Q. He, F. Chen, Z. Zhao, et al., Supramolecular mimotope peptide nanofibers promote antibody–ligand polyvalent and instantaneous recognition for biopharmaceutical analysis, Anal. Chem. 96 (2024) 5940–5950.
[39] J. Yang, A. Zhou, M. Li, et al., Mimotope peptide modified pompon mum-like magnetic microparticles for precise recognition, capture and biotransformation analysis of rituximab in biological fluids, Acta Pharm. Sin. B 14 (2024) 1317–1328.
[40] J. Zhou, C. Zuo, H. Tian, et al., Magnetic composite membrane roll column for rapid and high efficiency separation of antibodies, Sep. Purif. Technol. 309 (2023), 123107.
[41] S. Huang, M. Zhang, F. Chen, et al., A chimeric hairpin DNA aptamer-based biosensor for monitoring the therapeutic drug bevacizumab, Analyst 149 (2024) 212–220.
[42] Q. Luo, H. Zou, Q. Zhang, et al., High-performance affinity chromatography with immobilization of protein A and L-histidine on molded monolith, Biotechnol. Bioeng. 80 (2002) 481–489.
[43] W. Liu, A.L. Bennett, W. Ning, et al., Monoclonal antibody capture and analysis using porous membranes containing immobilized peptide mimotopes, Anal. Chem. 90 (2018) 12161–12167.
[44] L. Huang, J. Lu, V.J. Wroblewski, et al., *In vivo* deamidation characterization of monoclonal antibody by LC/MS/MS, Anal. Chem. 77 (2005) 1432–1439.
[45] S. Yin, C.V. Pastuskovas, L.A. Khawli, et al., Characterization of therapeutic monoclonal antibodies reveals differences between *in vitro* and *in vivo* time-course studies, Pharm. Res. 30 (2013) 167–178.